# His-tags as Zn(II) binding motifs in a protein-based fluorescent sensor

Please check the document version of this publication:

• A submitted manuscript is the version of the article upon submission and before peer-review. There can be important differences between the submitted version and the official published version of record. People interested in the research are advised to contact the author for the final version of the publication, or visit the DOI to the publisher's website.
• The final author version and the galley proof are versions of the publication after peer review.
• The final published version features the final layout of the paper including the volume, issue and page numbers.

[Link to publication](#)

# His-tags as Zn(II) binding motifs in a protein-based fluorescent sensor

Toon H. Evers, Marieke A.M. Appelhof, E.W. Meijer and Maarten Merkx[1]

Laboratory of Chemical Biology, Department of Biomedical Engineering, Eindhoven University of Technology, PO Box 513, 5600 MB Eindhoven, The Netherlands

[1]To whom correspondence should be addressed. E-mail: m.merkx@tue.nl

**Fluorescent indicators that allow real-time imaging of Zn(II) in living cells are invaluable tools for understanding Zn(II) homeostasis. Genetically encoded sensors based on fluorescence resonance energy transfer between fluorescent protein domains have important advantages over synthetic probes. We discovered that hexahistidine tags have a strong tendency to dimerize upon binding of Zn(II) in solution and we used this principle to develop a new protein-based sensor for Zn(II). Enhanced cyan and yellow fluorescent proteins were connected by long flexible peptide linkers and His-tags were incorporated at both termini of this fusion protein. The resulting sensor CLY9-2His allows the ratiometric fluorescent detection of Zn(II) in the nanomolar range. In addition, CLY9-2His is selective over the physiologically relevant metal ions Fe(II), Mn(II), Ca(II) and Mg(II). Our approach demonstrates the potential of using small peptides as metal-binding ligands in chelating fluorescent protein chimeras.**
*Keywords*: fluorescent probes/FRET/GFP/hexahistidine tag/ Zn(II) sensor

## Introduction

Zinc is the second most abundant transition metal in the human body and is essential to a wide variety of cellular processes. This redox stable metal is a structural cofactor in, for example, transcription factors, performs a catalytic role as a Lewis acid in enzymes and functions as a neuromodulator (Berg and Shi, 1996; Lipscomb and Sträter, 1996; Frederickson *et al*., 2005; Mocchegiani *et al*., 2005). Despite its abundance, almost all intracellular Zn(II) is bound by proteins and intracellular free Zn(II) concentrations are estimated to be subnanomolar in mammalian cells (Simons, 1991a, 1991b; Adebodun and Post, 1995; Finney and O'Halloran, 2003; Chang *et al*., 2004; Bozym *et al*., 2006). The intracellular concentration is thus tightly regulated and disruption of zinc homeostasis can lead to apoptosis or necrotic cell death (Frederickson *et al*., 2005; Mocchegiani *et al*., 2005). Furthermore, a role for Zn(II) has been implicated in neurodegenerative disorders such as Alzheimer's disease, Parkinson's disease, Creutzfeldt-Jakob disease and amyotrophic lateral sclerosis (Mocchegiani *et al*., 2005).

Since fluorescence microscopy is ideally suited to monitor cellular processes, fluorescent indicators for Zn(II) are attractive tools to study Zn(II) homeostasis in living cells with high spatial and temporal resolution. Many fluorescent sensors for chelatable Zn(II) have been developed, ranging from small membrane-permeable organic probes to peptide-based indicators and recently also genetically encoded sensor proteins (Jiang and Guo, 2004; Taki *et al*., 2004; Ajayaghosh *et al*., 2005; Kawabata *et al*., 2005; Thompson, 2005; Woodroofe *et al*., 2005; Bozym *et al*., 2006; Qiao *et al*., 2006; Royzen *et al*., 2006; Evers *et al*., 2007; van Dongen *et al*., 2007). The latter have the advantage that they do not require expensive and laborious synthesis, allow non-invasive imaging, can be targeted to different organelles and can be easily adapted by mutagenesis. Tsien and coworkers pioneered the concept of genetically encoded sensors by developing the Ca(II) sensor Cameleon (Miyawaki *et al*., 1997). Cameleon and similar protein-based sensors consist of a sensor domain that is sandwiched between two spectrally distinct fluorescent proteins, usually enhanced cyan and yellow fluorescent protein (ECFP and EYFP). When ECFP is excited, its excitation energy can be transferred to EYFP in a process called Förster or fluorescence resonance energy transfer (FRET) (Lakowicz, 1999). Because the energy transfer efficiency is dependent on the distance between ECFP and EYFP and their relative orientation, a conformational change in the sensor domain causes a change in the fluorescence emission of the sensor. Due to the use of two fluorophores in one molecule, the fluorescent response of this type of sensor is ratiometric and not dependent on the sensor concentration.

Recently, we and others reported the first examples of genetically encoded FRET-based sensor proteins for Zn(II) (Qiao *et al*., 2006; Evers *et al*., 2007; van Dongen *et al*., 2007). During the development of new types of Zn(II) sensors, we made the serendipitous discovery that a simple fusion protein of ECFP and EYFP also possessed a moderate affinity for Zn(II), but only when a hexahistidine tag (His-tag) was present at the N-terminus. Here we show that this effect is due to the Zn(II)-mediated dimerization of two His-tagged ECFP-linker-EYFP proteins. This knowledge was subsequently applied to construct single-protein sensors that contain His-tags at both the N- and C-terminus and a variety of linker lengths between ECFP and EYFP. Besides providing an attractive new sensor system for intracellular Zn(II) imaging, this work also yields new insights into the coordination chemistry of His-tags with metal ions in solution.

## Materials and methods

### Cloning of expression vectors for CLYx-2His, His-ECFP and EYFP-His

ECFP and EYFP used in this study were originally amplified from pECFP-C1 and pEYFP-N1 vectors (Clontech). All oligonucleotides were purchased from MWG Biotech and restriction enzymes were obtained from New England Biolabs. The construction of the expression vector for His-CLY9, pET28-CLY9, was described before (Evers *et al*., 2006). Mutation of the stop codon in pET28-CLY9 to

introduce a C-terminal His-tag was complicated by the large sequence similarity between the ECFP and EYFP genes. The expression vector for CLY9-2His (pET28-CLY9-2His) was therefore obtained by first removing the stop codon in pET28-WD4-YFP (van Dongen *et al.*, 2006) using the QuikChange Site-Directed Mutagenesis Kit (Stratagene) and the following primers: 5′-GAGTGCGGCCGCTTTCTTGTA CAGCTCGTC-3′ and 5′-GACGAGCTGTACAAGAAAGCG GCCGCACTC-3′, resulting in pET28-WD4-YFP-His. Subsequently, the sequence encoding EYFP was removed from pET28-CLY9 and replaced by DNA encoding EYFP with a C-terminal His-tag from pET28-WD4-YFP-His using *Blp* I and *Pst* I restriction sites, resulting in pET28-CLY9-2His. Because the GGSGGS repeats in the linker sequence are separated by *BamH* I restriction sites, the expression vectors pET28-CLYx-2His (where x indicates the number of GGSGGS repeats in the linker) could be easily obtained by a partial digestion and religation procedure as described before (Evers *et al.*, 2006). After transformation of *Escherichia coli* NovaBlue (Novagen) with the ligation mixture, colony PCR was used to identify clones containing pET28-CLY1-2His and pET28-CLY5-2His. The expression vector for EYFP-His (pET28-EYFP-His) was obtained after removing the sequence encoding WD4 from pET28-WD4-YFP-His by digestion with *Nco*I and religation of the vector. The expression vector for His-ECFP (pET28-ECFP) was created by introducing a stop codon after the DNA encoding ECFP in pET28-CFP-ATOX (Van Dongen *et al.*, 2006) using the following primers: 5′-GCTTCGGCATTC CTCACTTGTACAGCTCG-3′ and 5′-CGAGCTGTACAAGT GAGGAATGCCGAAGC-3′. The correct open reading frames for all constructs were confirmed by DNA sequencing (BaseClear).

### Protein expression and purification

Expression of His-CLY9, His-ECFP, EYFP-His and CLYx-2His was performed essentially as described before (Evers *et al.*, 2006). Briefly, proteins were isolated from *E. coli* BL21(DE3) cells and purified using nickel affinity chromatography on His-bind resin (Novagen). If necessary, proteins were further purified using size exclusion chromatography on a Sephacryl S-200 HR column (GE Healthcare), equilibrated with 50 mM Tris/HCl, 100 mM NaCl, pH 8.0. To remove the N-terminal His-tags of His-CLY9 and CLY9-2His, these proteins were dialyzed against 20 mM Tris/HCl, 150 mM NaCl, 2.5 mM CaCl₂, pH 8.4 using 12– 14 kDa molecular weight cutoff dialysis membranes (Spectropore). Subsequently, 1 U thrombin/mg protein (Novagen) was added to the protein solution and incubated for 24 h at 4°C. The resulting proteins CLY9 and CLY9-His were purified from the cleaved His-tag using size exclusion chromatography as described above. All CLYx-2His proteins showed the absorption bands typical of ECFP and EYFP at the ratio that is expected when both domains are fully folded. Final protein preparations were dialyzed against 50 mM Tris/HCl, 100 mM NaCl, pH 8.0 and stored at −80°C.

### Spectroscopy

UV-vis spectra were recorded on a Shimadzu Multispec 1501 photodiode array spectrometer. Protein concentrations were determined using molar extinction coefficients of 84 000 M⁻¹ cm⁻¹ at 514 nm for EYFP-His, CLY9, His-CLY9, CLY9-His and CLYx-2His (Patterson *et al.*, 2001) and 29 000 M⁻¹ cm⁻¹ at 434 nm for His-ECFP (Rizzo *et al.*, 2004). For all fluorescence measurements, protein samples were briefly treated with 4 M urea to disrupt the possible formation of aggregates. Urea was subsequently removed by passing the protein solution two times through a Zeba desalt spin column (Pierce), equilibrated with 50 mM Tris/HCl, 100 mM NaCl, 10% (v/v) glycerol, 0.05% (v/v) Tween-20, pH 8.0. Fluorescence measurements were performed on a Varian Cary Eclipse fluorescence spectrometer, fitted with horizontal and vertical polarizers in a fast filter wheel setup. Protein solutions were kept at 20°C by a Varian single cell Peltier accessory. Fluorescence emission spectra were recorded from 450 to 600 nm using 420 nm excitation and corrected for the wavelength-dependent efficiency of the instrument. Emission spectra were normalized using the emission intensity at 527 nm after 500 nm excitation. From these normalized spectra, the amount of FRET was expressed either as the EYPF/ECFP emission ratio $R_{527/475}$ (the emission intensity at 527 nm divided by the emission ratio at 475 nm) or as the difference between the emission intensities at 527 and 475 nm $(I_{527} - I_{475})$. Emission anisotropy measurements were performed using the automated polarization measurements ADL program (Varian), using polarized excitation light of 500 nm and recording the emission from 525.5 to 528.5 nm with 0.15 nm steps. Anisotropy values were calculated by averaging the anisotropy values obtained at each wavelength.

### Zn(II) titrations

All Zn(II) titrations were performed using freshly prepared, slightly acidic stock solutions of ZnCl₂ (Sigma-Aldrich). After each addition, emission spectra were recorded and anisotropy measurements were performed as described above. For CLY9, His-CLY9 and CLY9-His, 6–1120 μM Zn(II) was added to a 0.5 μM protein solution in 50 mM Tris/HCl, 100 mM NaCl, 10% (v/v) glycerol, 0.05% (v/v) Tween-20, pH 8.0. The emission difference $I_{527} - I_{475}$ as a function of the Zn(II) concentration was fit with GraphPad Prism 4.0 using:

$$I_{527} - I_{475} = A + B \left\{ [\text{protein}]_{\text{total}} + 1/K_A[\text{Zn(II)}]_{\text{free}} \right.$$
$$\left. - \sqrt{(-[\text{protein}]_{\text{total}} - 1/K_A[\text{Zn(II)}]_{\text{free}})^2 - [\text{protein}]_{\text{total}}^2} \right\} / 2$$

$$(1)$$

in which $A$ and $B$ are constants to fit the fluorescence intensity, $K_A$ is the overall formation constant of the formation of the ternary complex, $[\text{protein}]_{\text{total}} = 0.5 \times 10^{-6}$ M and $[\text{Zn(II)}]_{\text{free}} = [\text{Zn(II)}]_{\text{total}}$ (van Dongen *et al.*, 2006). For His-ECFP and EYFP-His, 6–1120 μM Zn(II) was added to a solution containing 0.5 μM of both proteins in 50 mM Tris/ HCl, 100 mM NaCl, 10% (v/v) glycerol, 0.05% (v/v) Tween-20, pH 8.0. $I_{527} - I_{475}$ as a function of the Zn(II) concentration was fit using Eq. (1) with $[\text{protein}]_{\text{total}} = 1 \times 10^{-6}$ M and $[\text{Zn(II)}]_{\text{free}} = [\text{Zn(II)}]_{\text{total}}$. For CLY1-2His, CLY5-2His and CLY9-2His, titrations at low Zn(II) concentrations were performed at 50 nM protein concentration in a buffering system consisting of 50 mM Tris/HCl, 100 mM NaCl, 10%

(v/v) glycerol, 0.05% (v/v) Tween-20, pH 8.0, supplemented with 1 mM EGTA, 10 mM Ba(II) and 0.05–0.9 mM Zn(II). Free Zn(II) concentrations were calculated using the MaxChelator program (Patton *et al.*, 2004). $I_{527} - I_{475}$ as a function of the Zn(II) concentration was fit using Eq. (2), where $K_d$ is the dissociation constant for the protein-Zn(II) complex and $A$ and $B$ are constants to fit the fluorescence intensity:

$$I_{527} - I_{475} = A + B[\text{metal}]_{\text{free}}/(K_d + [\text{metal}]_{\text{free}}) \quad (2)$$

### Determination of metal selectivity

Metal additions were performed from stock solutions of $BaCl_2$ (Acros), $CoSO_4$, $CaCl_2$ (Merck), $Fe(NH_4)_2(SO_4)_2$, $MnSO_4$, $MgSO_4$, $NiSO_4$ and $Cd(OAc)_2$ (Sigma-Aldrich) in water. Pb(II) was diluted from a 1000 μg/ml lead atomic standard solution (Sigma-Aldrich). Fluorescence emission spectra were recorded after addition of 20 μM Ni(II), Cd(II), Co(II), Cu(II), Fe(II), Mn(II) and Pb(II) or 10 mM Ba(II), Ca(II) or Mg(II) to a 50 nM solution of CLY9-2His in 50 mM Tris/HCl, 100 mM NaCl, 10% (v/v) glycerol, 0.05% (v/v) Tween-20, pH 8.0. After addition of 1 μM Zn(II) to these samples, the emission spectrum was recorded again and $R_{527/475}$ was calculated.

### Ni(II) titrations

Ni(II) titrations were performed by addition of 0.2–1250 μM $NiSO_4$ to a 50 nM solution of CLY9-2His in 50 mM Tris/HCl, 100 mM NaCl, 10% (v/v) glycerol, 0.05% (v/v) Tween-20, pH 8.0 and emission spectra and anisotropy were recorded after each addition. The fluorescent response ($I_{527} - I_{475}$) from 0 to 9 μM Ni(II) was fit using Eq. (2), assuming that $[\text{Ni(II)}]_{\text{free}} = [\text{Ni(II)}]_{\text{total}}$.

## Results

### Zn(II)-mediated dimerization of His-tagged proteins

We recently reported the construction of a new ratiometric Zn(II) sensor protein called ZinCh-x by introduction of two Zn(II) binding amino acids (Y39H and S208C) at the dimerization interface of both fluorescent protein domains in an ECFP-linker-EYFP fusion protein (Evers *et al.*, 2007). The flexible linker separating the two fluorescent domains in these chimeras consisted of x GGSGGS repeats, with x = 1–9. The precursor proteins for these fusion proteins contain an N-terminal hexahistidine sequence that allows easy purification, but which is normally removed by cleavage with thrombin. During this work, we noticed that CFP-linker-YFP (CLY) without the Zn(II) binding mutations also displayed an increase in FRET in the presence of Zn(II) when the His-tag was not removed after protein purification. Figures 1A and B show that this protein, His-CLY9, displayed a large increase in the EYFP/ECFP emission ratio ($R_{527/475}$) in the presence of micromolar concentrations of Zn(II). Removal of the His-tag abolished this effect, showing that the His-tag was involved in this specific Zn(II) binding. To further study the nature of the conformational change upon Zn(II) binding, the fluorescence emission anisotropy of the EYFP domain of His-CLY9 was monitored during a Zn(II) titration (Fig. 1C). In the absence of Zn(II), His-CLY9 displayed a high anisotropy of 0.34. This value is equal to
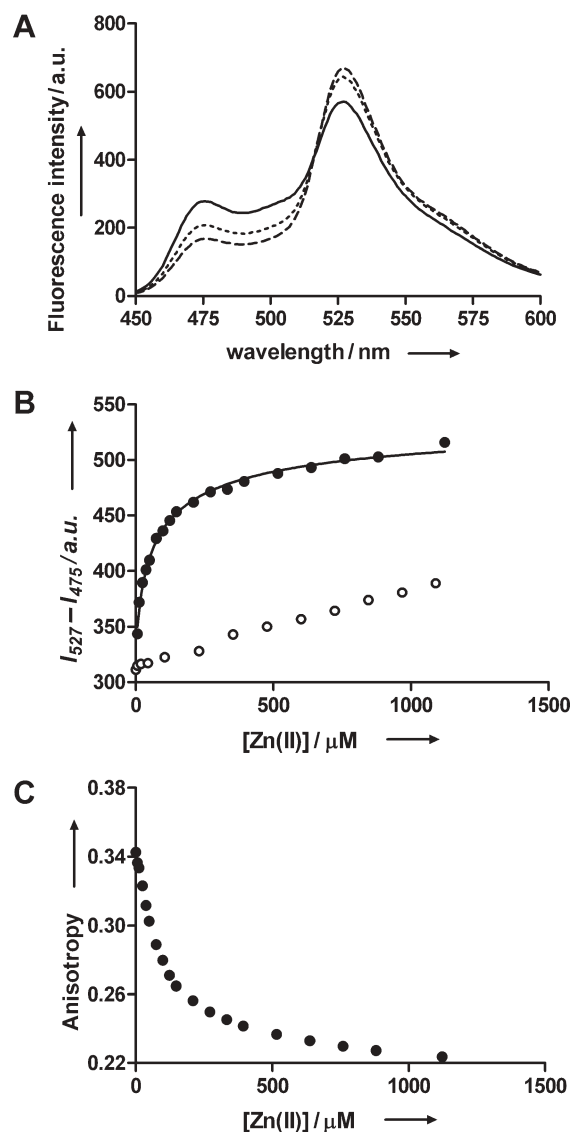


**Fig. 1.** (**A**) Fluorescence emission spectra of 0.5 μM His-CLY9 in 50 mM Tris/HCl, 100 mM NaCl, 10% (v/v) glycerol, 0.05% (v/v) Tween-20, pH 8.0 in the absence (solid line) and in the presence of 100 μM (dotted line) and 900 μM Zn(II) (dashed line). (**B**) Zn(II) titration for 0.5 μM His-CLY9 (filled circles) or CLY9 (open circles) showing the difference in fluorescence intensities at 527 and 475 nm ($I_{527} - I_{475}$), using 420 nm excitation. The solid line is a fit of the data using Eq. (1) and $K_A = 7.7 \pm 1.1 \times 10^{10} \text{ M}^{-2}$. (**C**) Zn(II) titration showing the EYFP emission anisotropy after direct excitation of the EYFP domain of His-CLY9.

that measured for single EYFP, indicating that the rotational diffusion of the protein domain is unaffected by the fusion with the ECFP domain (Evers *et al.*, 2006; Vinkenborg *et al.*, 2007). In the presence of Zn(II), a strong decrease in anisotropy was observed. The only plausible explanation for this enhanced depolarization is energy transfer from one EYFP domain to another, differently oriented EYFP domain (homotransfer). The Förster distance for the EYFP–EYFP pair is 51Å (Patterson *et al.*, 2000), which means that His-CLY9 most likely dimerized upon binding of Zn(II). Because the His-tags are essential for Zn(II) binding, we concluded that the His-tags of His-CLY9 dimerize in the presence of Zn(II), forming the complex depicted in Fig. 2A. The increase in energy transfer between ECFP and EYFP in this complex is due to the presence of a second, intermolecular energy
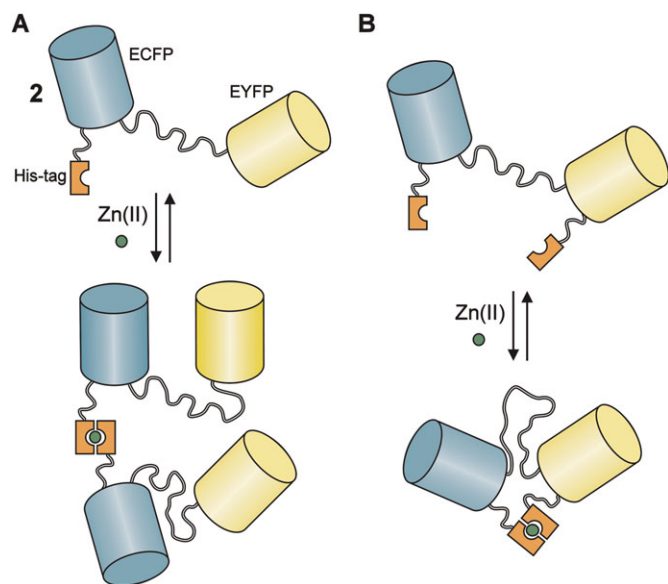
**Fig. 2.** (**A**) Proposed structure of the His-CLY9 dimer that is formed upon Zn(II) binding. Each His-CLY9 protein consists of ECFP connected to EYFP by a flexible linker and contains an N-terminal His-tag. Two His-tags are required for the effective binding of one or more Zn(II) ions, causing the protein to dimerize and resulting in an increase in FRET from ECFP to EYFP and homo-FRET between EYFP domains. (**B**) Design of CLY9-2His containing both an N-terminal and a C-terminal His-tag. Introduction of two His-tags in a single protein results in the formation of a compact, intramolecular Zn(II) complex with an increased affinity for Zn(II) due to the chelate effect.

transfer pathway. Assuming the formation of a 2:1 His-CLY9:Zn(II) complex, the increase in energy transfer could be fit well with an apparent association constant $K_A$ of $7.7 \pm 1.1 \times 10^{10}$ M$^{-2}$ (Fig. 1B).

### A new sensor design based on Zn(II)-induced dimerization of His-tags

Based on the finding that His-tags dimerize in the presence of Zn(II), we reasoned that a chimera of ECFP and EYFP carrying a His-tag at both termini would display an enhanced affinity for Zn(II). The effective concentration of one His-tag with respect to the other can reach values in the millimolar range when both His-tags are located on the same molecule, which increases the likelihood of intramolecular complex formation (Zhou, 2003; Van Dongen *et al.*, 2007). Another advantage of such a single protein sensor is that the fluorescent response is not dependent on the protein concentration (Fig. 2B). Because the expression vector for His-CLY9 already contained a sequence encoding for a His-tag downstream of the EYFP gene, the deletion of a single base pair in the original stop codon was sufficient to create CLY9-2His, which contains an additional C-terminal KAAALEHHHHHH sequence.

The emission ratio of ∼2.1 that is observed for CLY9-2His in the absence of Zn(II) is the same as was previously reported for the same protein without His-tags (CLY9), which corresponds to an energy transfer efficiency of ∼45% (Evers *et al.*, 2006). The introduction of the His-tags as such did therefore not enhance the formation of intramolecular domain–domain interactions. Addition of 0.5 μM Zn(II) to CLY9-2His yielded a 1.6-fold increase in EYFP/ECFP emission ratio (Fig. 3A), corresponding to an

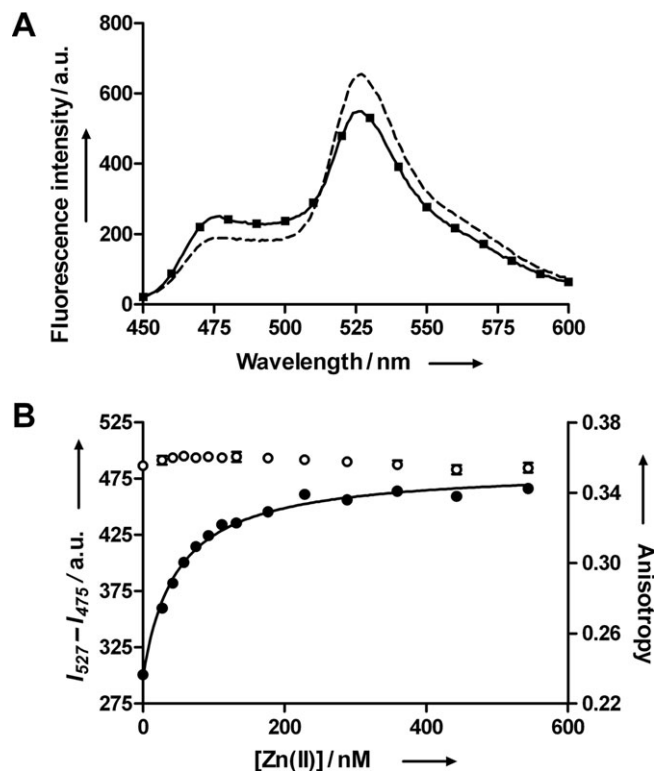**Fig. 3.** (**A**) Fluorescence emission spectra of CLY9-2His excited at 420 nm before (solid line) and after addition of 0.5 μM Zn(II) (dashed line) and an excess of EDTA (squares). (**B**) Zn(II) titration experiment for 50 nM CLY9-2His in 50 mM Tris/HCl, 100 mM NaCl, 10% (v/v) glycerol, 0.05% (v/v) Tween-20, pH 8.0, supplemented with 1 mM EGTA, 10 mM Ba(II) and 0.05–0.9 mM Zn(II) to obtain nanomolar free Zn(II) concentrations, showing the difference in fluorescence emission intensities at 527 and 475 nm after 420 nm excitation (filled circles) and the fluorescence emission anisotropy at 527 nm after 500 nm excitation (open circles). The solid line is a fit of the data using Eq. (2) with a $K_d$ of $47 \pm 4$ nM.

increase in energy transfer efficiency to ∼65%. Addition of an excess of EDTA to the Zn(II)-bound sensor completely reversed the change in fluorescence, indicating that Zn(II) binding is reversible. A Zn(II) titration using a Zn(II) buffering system revealed that CLY9-2His has a much higher Zn(II) affinity than His-CLY9. The fluorescent response could be fit by a simple 1:1 binding model, yielding a $K_d$ of $47 \pm 4$ nM for CLY9-2His (Fig. 3B). This large enhancement in affinity for Zn(II) is consistent with the preferred intramolecular association of the N- and C-terminal His-tags of CLY9-2His. Addition of Zn(II) to CLY9-2His did not affect its EYFP anisotropy, which also confirmed the formation of an intramolecular Zn(II) complex and the absence of dimer formation (Fig. 3B).

To allow careful comparison of the Zn(II) affinity for the intramolecular versus the intermolecular association of His-tags, we also produced the His-tagged fluorescent proteins without a connecting linker. A Zn(II) titration for a 1:1 mixture of ECFP with an N-terminal His-tag (His-ECFP) and EYFP with a C-terminal His-tag (EYFP-His) yielded an overall association constant of $5.3 \pm 0.9 \times 10^{10}$ M$^{-2}$ (Fig. 4A), similar to that for the formation of the Zn(II)-bridged His-CLY9 dimer. To investigate whether two C-terminal His-tags could also bind Zn(II) with the same affinity, the N-terminal His-tag of CLY9-2His was removed. The resulting protein CLY9-His also formed oligomers upon
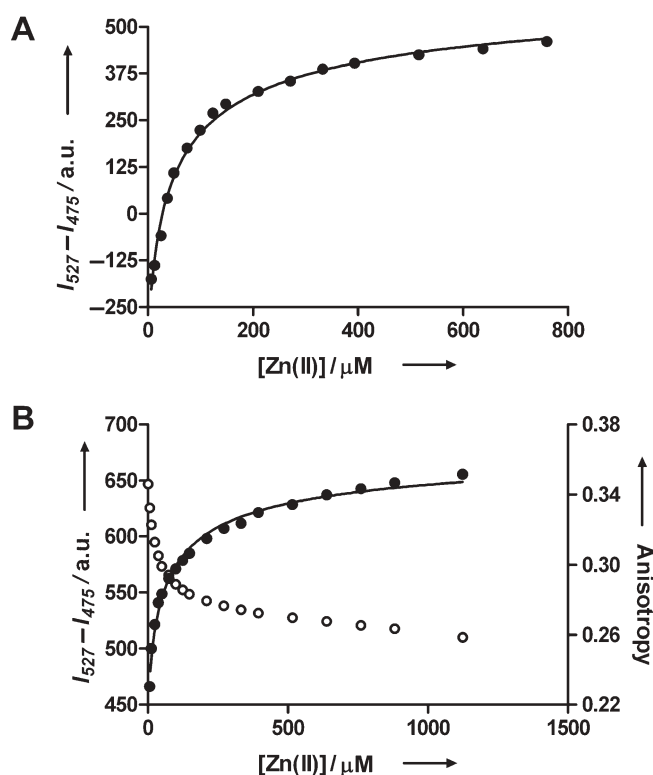
**Fig. 4.** (**A**) Zn(II) titration for a mixture of 0.5 μM His-ECFP and 0.5 μM EYFP-His in 50 mM Tris/HCl, 100 mM NaCl, 10% (v/v) glycerol, 0.05% (v/v) Tween-20, pH 8.0, showing the difference in fluorescence emission intensity at 527 and 475 nm. The solid line is a fit of the data using Eq. (1) and $K_A = 5.3 \pm 0.9 \times 10^{10}$ M$^{-2}$. (**B**) Zn(II) titration experiment for 0.5 μM CLY9-His in 50 mM Tris/HCl, 100 mM NaCl, 10% (v/v) glycerol, 0.05% (v/v) Tween-20, pH 8.0, showing $I_{527}-I_{475}$ (solid circles) and the EYFP anisotropy (open circles) as a function of Zn(II) concentration. The solid line is a fit of $I_{527}-I_{475}$ using Eq. (1) and $K_A = 8.5 \pm 1.5 \times 10^{10}$ M$^{-2}$.



**Fig. 5.** Linker length dependence of sensor properties, measured at 50 nM protein concentration in 50 mM Tris/HCl, 100 mM NaCl, 10% (v/v) glycerol, 0.05% (v/v) Tween-20, pH 8.0. (**A**) The EYFP/ECFP emission ratios for CLY1-2His, CLY5-2His and CLY9-2His in the absence (white bars) and the presence of 0.5 μM Zn(II). The corresponding relative ratio change (RRC) upon Zn(II) binding is indicated for each protein. (**B**) The dissociation constants of Zn(II) binding for CLY1-2His, CLY5-2His and CLY9-2His as determined from Zn(II) titration experiments, using Eq. (2) to fit the fluorescence emission differences $I_{527}-I_{475}$. The error bars represent the standard error of the fit.



**Fig. 6.** Determination of metal selectivity of CLY9-2His in 50 mM Tris/HCl, 100 mM NaCl, 10% (v/v) glycerol, 0.05% (v/v) Tween-20, pH 8.0. Gray bars represent the EYFP/ECFP emission ratio before the addition of metal (−) and after the addition of 20 μM Ni(II), Cd(II), Co(II), Cu(II), Fe(II), Mn(II), Pb(II) or 10 mM Ba(II), Ca(II) or Mg(II). After addition of the indicated metal, an addition of 1 μM Zn(II) was performed to determine whether the other metals could compete for Zn(II) binding to the His-tags (white bars).

binding of Zn(II) and displayed similar Zn(II) binding behavior ($K_A = 8.5 \pm 1.5 \times 10^{10}$ M$^{-2}$, Fig. 4B). This result shows that the location of the His-tag at either the N- or C-terminus of the protein did not influence the affinity for Zn(II).

### Dependence of ratio change and affinity on linker length

The length of the linker between the fluorescent domains can influence the difference in energy transfer efficiency between Zn(II)-bound and unbound states, but also determines the effective concentration of the Zn(II) binding sites. To determine the linker length dependence of the relative ratio change (RRC) and Zn(II) affinity, we also constructed sensors with 1 and 5 GGSGGS repeats in the flexible linker, CLY1-2His and CLY5-2His. In the absence of Zn(II), the fluorescence emission ratio decreased with increasing linker length (Fig. 5A). We previously showed that the corresponding energy transfer efficiencies can be quantitatively understood by modeling the linker as a random coil (Evers *et al.*, 2006), indicating that the sensor proteins are in an open conformation for all linker lengths. In the presence of Zn(II), the fluorescence emission ratio is increased for all proteins, but still shows a dependence on the linker length. The largest RRC, 1.6-fold, was obtained for the sensor with longest peptide linker, CLY9-2His. The affinity for Zn(II) was not significantly affected by the linker length, despite a difference of 48 residues in linker length between CLY9-2His and CLY1-2His (Fig. 5B).
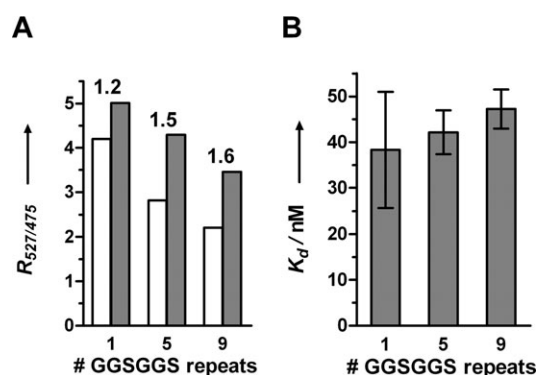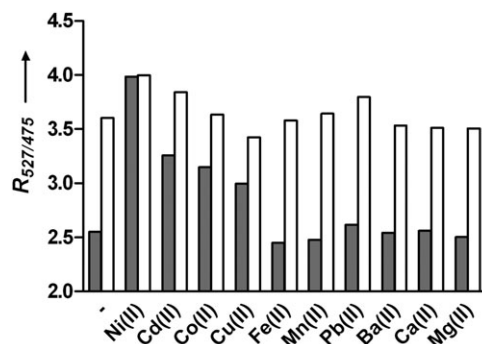
### Metal selectivity of CLY9-2His

The application of CLY9-2His in intracellular imaging applications not only requires a high affinity for Zn(II), but also selectivity over other physiologically relevant metals. To determine whether other metal ions could also mediate the dimerization of His-tagged protein domains, we monitored the change in fluorescence emission ratio of CLY9-2His after addition of a variety of divalent metal ions (Fig. 6). After each addition, 1 μM Zn(II) was added to determine which metal ions could effectively compete for Zn(II) binding to the His-tags. As was expected based on earlier reports of Ni(II) induced dimerization of His-tags (Sprules *et al.*, 1998; Stayner *et al.*, 2005), a large increase in $R_{527/475}$ was observed after addition of 20 μM Ni(II). Although less pronounced, addition of 20 μM Cd(II), Co(II) and Cu(II) also caused an increase in FRET. The latter two metal ions are commonly used in the immobilized metal affinity chromatography purification of His-tagged proteins. The affinity for
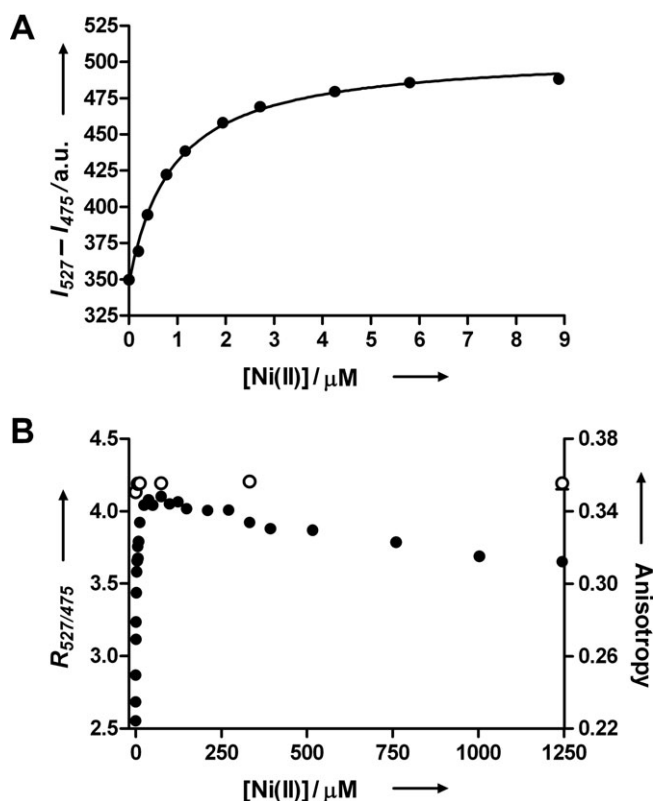
**Fig. 7.** Ni(II) titration experiments for 50 nM CLY9-2His in 50 mM Tris/HCl, 100 mM NaCl, 10% (v/v) glycerol, 0.05% (v/v) Tween-20, pH 8.0. (**A**) The fluorescent response to additions of 0.2–9 μM Ni(II) was fit with Eq. (2), yielding a $K_d$ of $8.8 \pm 0.7 \times 10^{-7}$ M. (**B**) The EYFP/ECFP emission ratio (filled circles) showed an increase at low Ni(II) concentration and a decrease at higher Ni(II) concentrations, whereas the anisotropy (open circles) only showed a small increase at low Ni(II) concentrations.

these metals seemed to be lower than for Zn(II), however, as subsequent addition of 1 μM Zn(II) still resulted in an appreciable increase in $R_{527/475}$. Other divalent metal ions such as Fe(II), Mn(II) and Pb(II) (all tested at 20 μM), or 10 mM of Ba(II), Ca(II) and Mg(II) did not compete for Zn(II) binding, as a subsequent addition of 1 μM Zn(II) caused a similar increase in $R_{527/475}$ as observed in the absence of other metals. Because Ni(II) was the only metal that could effectively compete with Zn(II) binding and because His-tagged proteins are often purified using immobilized Ni(II), we investigated the affinity for Ni(II) in more detail. A Ni(II) titration revealed a $K_d$ of $8.8 \pm 0.7 \times 10^{-7}$ M (Fig. 7A), showing that the affinity for Zn(II) is 20-fold higher than that for Ni(II). At low Ni(II) concentrations, the EYFP/ECFP emission ratio increased to similar values as observed for Zn(II)-bound CLY9-2His, but at higher Ni(II) concentrations a decrease in $R_{527/475}$ was observed (Fig. 7B). The EYFP anisotropy remained unchanged at 0.34 over the entire range of Ni(II) concentrations, which indicates that both the increase and decrease in FRET were the result of intramolecular conformational changes and not due to protein dimerization. The observed decrease in emission ratio could be due to Ni(II) binding to each of the two His-tags, thereby disrupting the Ni(II)-bridged dimer. In contrast, a similar decrease in emission ratio was not observed at high Zn(II) concentrations (data not shown).

## Discussion

Since its introduction by Hochuli and coworkers, the hexa-histidine tag has become one of the most widely used tags for protein purification (Hochuli *et al.*, 1988; Gaberc-Porekar and Menart, 2001). Although commonly used in combination with Ni(II) ions immobilized on a support containing nitrilotriacetic acid (NTA) groups (Hochuli *et al.*, 1987), its imidazole moieties can also bind to free coordination sites of immobilized Cu(II), Co(II) and Zn(II) (Casey *et al.*, 1995; Pasquinelli *et al.*, 2000; Gaberc-Porekar and Menart, 2001). In these complexes, the immobilized chelating group provides three or four ligands to the metal ion, while two or three adjacent histidines of the His-tag complete the octahedral coordination shell (Chen *et al.*, 2000; Kruppa and König, 2006). Our results show that in solution Zn(II) prefers coordination by two His-tags, probably because occupation of all coordination sites by a single His-tag is sterically unfavorable. Besides its use in protein purification, there are a growing number of applications that take advantage of the metal affinity of this genetic tag. For example, His-tags have been used for the selective and oriented immobilization of proteins on surfaces functionalized with metal chelating groups (Scbmitt *et al.*, 1994; Shnek *et al.*, 1994; Nieba *et al.*, 1997; Ueda *et al.*, 2003; Xu *et al.*, 2004; Abad *et al.*, 2005; Johnson and Martin, 2005; Lata and Piehler, 2005). In a similar manner, His-tagged proteins can be specifically and reversibly labeled with, for example, a metal chelating biotin or fluorophore (O'Shannessy *et al.*, 1995; Kapanidis *et al.*, 2001; Lata *et al.*, 2005; Goldsmith *et al.*, 2006). To improve the stability of these complexes, several groups have explored the use of multivalent interactions using multivalent NTA ligands (Lata *et al.*, 2005; Ojida *et al.*, 2006; Kim *et al.*, 2007) and/or proteins with multiple His-tags (Khan *et al.*, 2006). However, the results reported here suggest that adventitious Zn(II) in buffers or leaching of immobilized Ni(II) could cause an intramolecular interaction between two His-tags within the same protein, which might severely attenuate the binding properties of such proteins.

The high affinity of these Zn(II) sensors is based on the chelate effect. Because both His-tags are located on the same molecule, their high apparent or effective concentration promotes complex formation, resulting in an enhanced apparent affinity. The effective concentration $c_{eff}$ is related to the enhancement in apparent affinity by:

$$c_{eff} = \frac{K_A^f}{K_A^s} \quad (3)$$

where $K_A^f$ and $K_A^s$ are the overall association constants of Zn(II) binding by the covalently linked and separate proteins, respectively. From the observed apparent formation constants for Zn(II) binding by the separate proteins ($K_A^s = 5.3 \times 10^{10}$ M$^{-2}$) and CLY9-2His ($K_A^f = 2.1 \times 10^7$ M$^{-1}$), an effective concentration of $4.0 \times 10^{-4}$ M can be calculated. This value is only slightly lower than the values in the millimolar range that we recently determined for a Zn(II) sensor using the same linker length (van Dongen *et al.*, 2007).

The use of small peptides instead of protein domains for target recognition should allow the fluorescent domains to come in close proximity upon target binding and thus result in a large change in fluorescence. An explanation for the

relatively modest change in emission ratio that is observed upon Zn(II) binding to CLY9-2His is that the intervening sequences between the His-tags and the protein domains provide additional spacing between the protein domains in the Zn(II)-bound state. There are 10 residues located between the N-terminal His-tag and ECFP and 15 residues between EYFP and the C-terminal His-tag. Therefore, the protein does not adopt a fixed conformation upon binding of Zn(II), which is also reflected in the linker length dependence of the fluorescence emission ratio in the Zn(II)-bound state. Efforts to obtain a well-defined Zn(II)-bound conformation, e.g. by placement of the His-tags at other positions (Paramban et al., 2004) or by shortening the peptide spacers between the His-tags and the fluorescent domains, are therefore predicted to result in a larger change in the fluorescence emission ratio. Another possibility to improve the ratiometric change is changing the relative orientation of the chromphores by using circular permutants of the fluorescent domains (Baird et al., 1999; Nagai et al., 2004). For in vivo application, the sensors could be further improved by the use of new GFP variants such as Cerulean, which unlike ECFP has a single exponential decay time (Rizzo et al., 2004), and Citrine, which is more pH stable compared to EYFP (Shaner et al., 2005).

In the current sensor design, the intrinsic affinity of His-tags for Zn(II) combined with a high effective concentration have resulted in a $K_d$ of 47 nM, even though the His-tags were not in any way designed or optimized for the binding of free Zn(II). The Zn(II) affinity of CLY-2His is slightly higher than that of ZinCh, but still considerably weaker than that of two other recently developed genetically encoded FRET-based Zn(II) sensors. Eide and coworkers constructed a sensor with low nanomolar affinity for Zn(II) by flanking two zinc finger domains by ECFP and EYFP (Qiao et al., 2006). Our group reported a Zn(II) sensor with a tunable femtomolar to picomolar affinity (van Dongen et al., 2007), based on the Zn(II)-induced dimerization of the copper chaperones Atox1 and WD4 (van Dongen et al., 2006). While the latter sensors may be more suitable to probe the subnanomolar cytosolic concentrations of free Zn(II) under normal cellular conditions (Simons, 1991a, 1991b; Adebodun and Post, 1995; Outten and O'Halloran, 2001; Chang et al., 2004; Bozym et al., 2006), higher concentrations have been reported for specific cell types, and organelles, or after various stimuli (Zalewski et al., 1993; Brand and Kleineke, 1996; Sensi et al., 1997; Canzoniero et al., 1999; Sensi et al., 1999). For example, elevated extracellular Zn(II) concentrations in nerve tissue (Assaf and Chung, 1984) can result in intracellular free Zn(II) concentrations ranging from 35 nM to several micromolar (Koh et al., 1996; Sensi et al., 1997; Canzoniero et al., 1999; Sensi et al., 1999). Furthermore, after oxidative stress or during apoptosis, Zn(II) can be released from cellular stores like presynaptic boutons or metallothionein (Zalewski et al., 1994; Aizenman et al., 2000; Maret, 2000; Truong-Tran et al., 2001; Frederickson et al., 2002; Spahl et al., 2003). In contrast to other genetically encoded sensors that rely on cysteines for Zn(II) binding, Zn(II) binding to CLY9-2His relies solely on histidine residues, making this sensor redox-insensitive. An important issue that remains to be addressed is how fast the sensor response is, as this will determine its suitability for intracellular monitoring of Zn(II) fluctuations in, for example, neuronal cells. Finally, several possibilities to improve both the affinity and the selectivity of the current sensor can be envisioned. The number of histidine residues and also their spacing could be adapted to improve the binding characteristics (Pasquinelli et al., 2000). Alternatively, phage display peptide libraries could be screened for alternative tags with enhanced metal selectivity.

## Conclusion

We have developed a genetically encoded fluorescent sensor for Zn(II) based on the Zn(II)-induced dimerization of His-tags. CLY9-2His as a genetically encoded sensor is unique in its use of small peptides for target recognition. An important advantage of using peptides instead of proteins as the sensor domain is that peptide display techniques can be applied to select peptide pairs with a higher Zn(II) affinity from large peptide libraries. For example, phage display has been used to select peptides that can bind immobilized Cu(II) (Patwardhan et al., 1997) or Ni(II) (Patwardhan et al., 1998) and fimbria display has revealed novel Zn(II) chelating peptides (Kjærgaard et al., 2001). The approach described here for Zn(II) could thus be extended for other targets by incorporation of these phage display-derived peptide sequences into chelating fluorescent protein chimeras.

## Acknowledgements

## References

Abad,J.M., Mertens,S.F.L., Pita,M., Fernández,V.M. and Schiffrin,D.J. (2005) *J. Am. Chem. Soc.*, **127**, 5689–5694.

Adebodun,F. and Post,J.F.M. (1995) *J. Cell. Physiol.*, **163**, 80–86.

Aizenman,E., Stout,A.K., Hartnett,K.A., Dineley,K.E., McLaughlin,B. and Reynolds,I.J. (2000) *J. Neurochem.*, **75**, 1878–1888.

Ajayaghosh,A., Carol,P. and Sreejith,S. (2005) *J. Am. Chem. Soc.*, **127**, 14962–14963.

Assaf,S.Y. and Chung,S.H. (1984) *Nature*, **308**, 734–736.

Baird,G.S., Zacharias,D.A. and Tsien,R.Y. (1999) *Proc. Natl Acad. Sci. USA*, **96**, 11241–11246.

Berg,J.M. and Shi,Y. (1996) *Science*, **271**, 1081–1085.

Bozym,R.A., Thompson,R.B., Stoddard,A.K. and Fierke,C.A. (2006) *ACS Chem. Biol.*, **1**, 103–111.

Brand,I.A. and Kleineke,J. (1996) *J. Biol. Chem.*, **271**, 1941–1949.

Canzoniero,L.M., Turetsky,D.M. and Choi,D.W. (1999) *J. Neurosci.*, **19**, 31.

Casey,J.L., Keep,P.A., Chester,K.A., Robson,L., Hawkins,R.E. and Begent,R.H.J. (1995) *J. Immunol. Methods*, **179**, 105–116.

Chang,C.J., Jaworski,J., Nolan,E.M., Sheng,M. and Lippard,S.J. (2004) *Proc. Natl Acad. Sci. USA*, **101**, 1129–1134.

Chen,Y., Pasquinelli,R., Ataai,M., Koepsel,R.R., Kortes,R.A. and Shepherd,R.E. (2000) *Inorg. Chem.*, **39**, 1180–1186.

Evers,T.H., van Dongen,E.M.W.M., Faesen,A.C., Meijer,E.W. and Merkx,M. (2006) *Biochemistry*, **45**, 13183–13192.

Evers,T.H., Appelhof,M.A.M., de Graaf-Heuvelmans,P.T.H.M., Meijer,E.W. and Merkx,M. (2007) *J. Mol. Biol.*, **374**, 411–425.

Finney,L.A. and O'Halloran,T.V. (2003) *Science*, **300**, 931–936.

Frederickson,C.J., Cuajungco,M.P., Labuda,C.J. and Suh,S.W. (2002) *Neuroscience*, **115**, 471–474.

Frederickson,C.J., Koh,J.-Y. and Bush,A.I. (2005) *Nat. Rev. Neurosci.*, **6**, 449–462.

Gaberc-Porekar,V. and Menart,V. (2001) *J. Biochem. Biophys. Methods*, **49**, 335–360.

Goldsmith,C.R., Jaworski,J., Sheng,M. and Lippard,S.J. (2006) *J. Am. Chem. Soc.*, **128**, 418–419.

Hochuli,E., Döbeli,H. and Schacher,A. (1987) *J. Chromatogr., A*, **411**, 177–184.

Hochuli,E., Bannwarth,W., Dobeli,H., Gentz,R. and Stuber,D. (1988) *Bio/Technology*, **6**, 1321–1325.

Jiang,P. and Guo,Z. (2004) *Coord. Chem. Rev.*, **248**, 205–229.

Johnson,D.L. and Martin,L.L. (2005) *J. Am. Chem. Soc.*, **127**, 2018–2019.

Kapanidis,A.N., Ebright,Y.W. and Ebright,R.H. (2001) *J. Am. Chem. Soc.*, **123**, 12123–12125.

Kawabata,E., Kikuchi,K., Urano,Y., Kojima,H., Odani,A. and Nagano,T. (2005) *J. Am. Chem. Soc.*, **127**, 818–819.

Khan,F., He,M. and Taussig,M.J. (2006) *Anal. Chem.*, **78**, 3072–3079.

Kim,J.S., Valencia,C.A., Liu,R.H. and Lin,W.B. (2007) *Bioconjug. Chem.*, **18**, 333–341.

Kjærgaard,K., Schembri,M.A. and Klemm,P. (2001) *Appl. Environ. Microbiol.*, **67**, 5467–5473.

Koh,J.-Y., Suh,S.W., Gwag,B.J., He,Y.Y., Hsu,C.Y. and Choi,D.W. (1996) *Science*, **272**, 1013–1016.

Kruppa,M. and König,B. (2006) *Chem. Rev.*, **106**, 3520–3560.

Lakowicz,J.R. (1999) *Principles of Fluorescence Spectroscopy*. Kluwer Academic/Plenum Publishers, New York.

Lata,S. and Piehler,J. (2005) *Anal. Chem.*, **77**, 1096–1105.

Lata,S., Reichel,A., Brock,R., Tampé,R. and Piehler,J. (2005) *J. Am. Chem. Soc.*, **127**, 10205–10215.

Lipscomb,W.N. and Sträter,N. (1996) *Chem. Rev.*, **96**, 2375–2433.

Maret,W. (2000) *J. Nutr.*, **130**, 1455S–1458S.

Miyawaki,A., Llopis,J., Heim,R., McCaffery,J.M., Adams,J.A., Ikura,M. and Tsien,R.Y. (1997) *Nature*, **388**, 882–887.

Mocchegiani,E., Malavolta,M., Bertoni-Freddari,C. and Marcellini,F. (2005) *Prog. Neurobiol.*, **75**, 367–390.

Nagai,T., Yamada,S., Tominaga,T., Ichikawa,M. and Miyawaki,A. (2004) *Proc. Natl Acad. Sci. USA*, **101**, 10554–10559.

Nieba,L., *et al.* (1997) *Anal. Biochem.*, **252**, 217–228.

O'Shannessy,D.J., O'Donnell,K.C., Martin,J. and Brigham-Burke,M. (1995) *Anal. Biochem.*, **229**, 119–124.

Ojida,A., Honda,K., Shinmi,D., Kiyonaka,S., Mori,Y. and Hamachi,I. (2006) *J. Am. Chem. Soc.*, **128**, 10452–10459.

Outten,C.E. and O'Halloran,T.V. (2001) *Science*, **292**, 2488–2492.

Paramban,R.I., Bugos,R.C. and Su,W.W. (2004) *Biotechnol. Bioeng.*, **86**, 687–697.

Pasquinelli,R.S., Shepherd,R.E., Koepsel,R.R., Zhao,A. and Ataai,M.M. (2000) *Biotechnol. Prog.*, **16**, 86–91.

Patterson,G.H., Piston,D.W. and Barisas,B.G. (2000) *Anal. Biochem.*, **284**, 438–440.

Patterson,G., Day,R. and Piston,D. (2001) *J. Cell. Sci.*, **114**, 837–838.

Patton,C., Thompson,S. and Epel,D. (2004) *Cell Calcium*, **35**, 427–431.

Patwardhan,A.V., Goud,G.N., Koepsel,R.R. and Ataai,M.M. (1997) *J. Chromatogr., A*, **787**, 91–100.

Patwardhan,A.V., Goud,G.N., Pasquinelli,R.S., Koepsel,R.R. and Ataai,M.M. (1998) *Biotechnol. Tech.*, **12**, 421–424.

Qiao,W., Mooney,M., Bird,A.J., Winge,D.R. and Eide,D.J. (2006) *Proc. Natl Acad. Sci. USA*, **103**, 8674–8679.

Rizzo,M.A., Springer,G.H., Granada,B. and Piston,D.W. (2004) *Nat. Biotechnol.*, **22**, 445–449.

Royzen,M., Durandin,A., Young,V.G., Jr, Geacintov,N.E. and Canary,J.W. (2006) *J. Am. Chem. Soc.*, **128**, 3854–3855.

Schmitt,L., Diefric,C. and Tampé,R. (1994) *J. Am. Chem. Soc.*, **116**, 8485–8491.

Sensi,S.L., Canzoniero,L.M.T., Yu,S.P., Ying,H.S., Koh,J.-Y., Kerchner,G.A. and Choi,D.W. (1997) *J. Neurosci.*, **17**, 9554–9564.

Sensi,S.L., Yin,H.Z., Carriedo,S.G., Rao,S.S. and Weiss,J.H. (1999) *Proc. Natl Acad. Sci. USA*, **96**, 2414–2419.

Shaner,N.C., Steinbach,P.A. and Tsien,R.Y. (2005) *Nat. Methods*, **2**, 905–909.

Shnek,D.R., Pack,D.W., Sasaki,D.Y. and Arnold,F.H. (1994) *Langmuir*, **10**, 2382–2388.

Simons,T.J.B. (1991a) *J. Membr. Biol.*, **123**, 73–82.

Simons,T.J.B. (1991b) *J. Membr. Biol.*, **123**, 63–71.

Spahl,D.U., Berendji-Grün,D., Suschek,C.V., Kolb-Bachofen,V. and Kröncke,D. (2003) *Proc. Natl Acad. Sci. USA*, **100**, 13952–13957.

Sprules,T., Green,N., Featherstone,M. and Gehring,K. (1998) *BioTechniques*, **25**, 20–22.

Stayner,R.S., Min,D.-J., Kiser,P.F. and Stewart,R.J. (2005) *Bioconjug. Chem.*, **16**, 1617–1623.

Taki,M., O'Halloran,T.V. and Wolford,J.L. (2004) *J. Am. Chem. Soc.*, **126**, 712–713.

Thompson,R.B. (2005) *Curr. Opin. Chem. Biol.*, **9**, 526–532.

Truong-Tran,A.Q., Carter,J., Ruffin,R.E. and Zalewski,P.D. (2001) *BioMetals*, **14**, 315–330.

Ueda,E.K.M., Gout,P.W. and Morganti,L. (2003) *J. Chromatogr. A*, **988**, 1–23.

van Dongen,E.M.W.M., Dekkers,L.M., Spijker,K., Meijer,E.W., Klomp,L.W.J. and Merkx,M. (2006) *J. Am. Chem. Soc.*, **128**, 10754–10762.

van Dongen,E.M.W.M., Evers,T.H., Dekkers,L.M., Meijer,E.W., Klomp,L.W.J. and Merkx,M. (2007) *J. Am. Chem. Soc.*, **129**, 3494–3495.

Vinkenborg,J.L., Evers,T.H., Reulen,S.W.A., Meijer,E.W. and Merkx,M. (2007) *ChemBioChem*, **8**, 1119–1121.

Woodroofe,C.C., Won,A.C. and Lippard,S.J. (2005) *Inorg. Chem.*, **44**, 3112–3120.

Xu,C., Xu,K., Gu,H., Zhong,X., Guo,Z., Zheng,R., Zhang,X. and Xu,B. (2004) *J. Am. Chem. Soc.*, **126**, 3392–3393.

Zalewski,P.D., Forbes,I.J. and Betts,W.H. (1993) *Biochem. J.*, **296**, 403–408.

Zalewski,P.D., Forbes,I.J., Seamark,R.F., Borlinghaus,R., Betts,W.H., Lincoln,S.F. and Ward,A.D. (1994) *Chem. Biol.*, **1**, 153–161.

Zhou,X. (2003) *J. Mol. Biol.*, **329**, 1–8.